Relativistic Shocks in Magnetized pair plasmas

Formation and short-term evolution

Illya Plotnikov

15.09.2016

Relativistic Shocks in Astrophysics (I)

	Ex. astro	Size scale	Flow Lorentz Γ
AGN	Cyg A	Mpc	2-20
Micro-Quasar	SS433	pc	≥ 1 (?)
Pulsar wind	Crab (M1)	pc	$10^3 - 10^7$
GRB	GRB 110731A	10^{-2}pc	~ 100

$$\Gamma = 1/\sqrt{1 - V^2/c^2}$$

- Universal presence of accretion disks and powerful jets.
- Radiate high energy photons (up to TeV energy)
- Accelerate particles above TeV/nucleon
- Amplify magnetic fields (or generate from scratch)

Jets : similar mechanism on different scales as origin of such shocks.

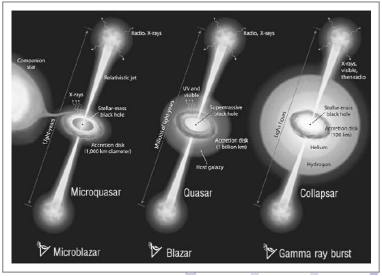

Relativistic Shocks in Astrophysics (II)

Crab Nebula (M1)

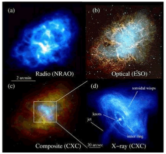

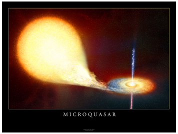

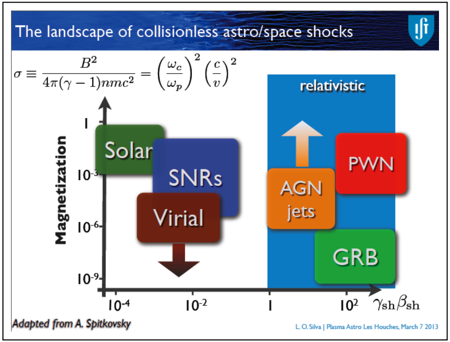

From L. Silva, Ecole des Houches, march 2013

M 87 : Virgo Galaxy

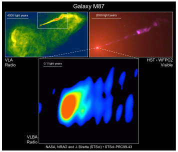

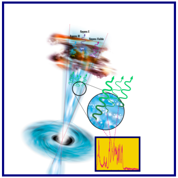

To the microphysics of shocks

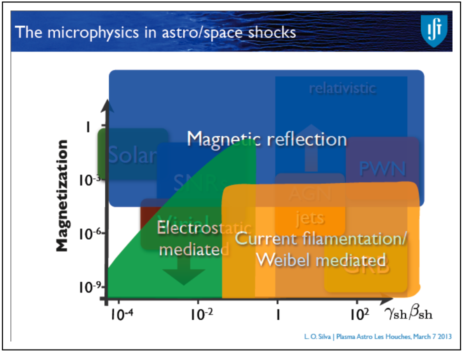

From L. Silva, Ecole des Houches, march 2013

→ Magnetization parameter (σ) : controls the shock structure and particle acceleration efficiency.

→ No complete theory of Magnetized relativistic collisionless shocks. While $\sigma = 0$ is well understood, and theoretical efforts in $0 < \sigma < 0.01$ limit (Lemoine & Pelletier 08,10 ; Plotnikov et al. 11,13 ; Lemoine et al. 13a,b), significant advances using PIC simulations (Sironi & Spitkovsky 09,11, Stockem et al 11, Sironi et al 13)...

Acceleration at shocks : Fermi I mechanism

Shocks : convergent flows with frozen-in magnetic turbulence.
Gain by cycles on both sides of the shock.

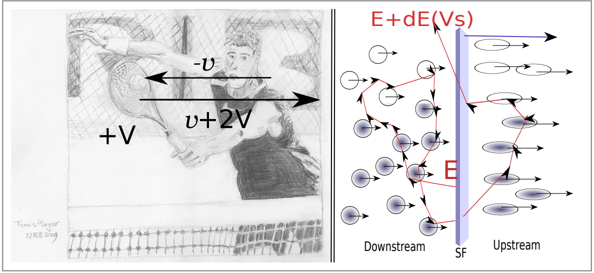

Krimsky 77, Axford et al. 77, Blandford & Ostriker 78, Bell 78 :
Diffusive Shock Acceleration by Fermi I mecanism : power-law particle distibution $f(E) \propto E^{-s}$, with $s \simeq 2$ (2.2 for UR shocks Achterberg et al. 01)

Evidenced in long-term 2D-3D PIC simulations of rel. shocks (e.g. Spitkovsky 08, Martins et al. 09, Haugbolle 2011)

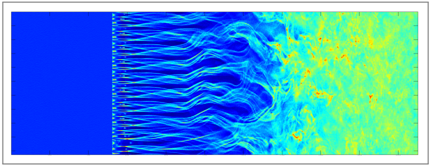

Simulation codes

Two types of codes used : FDTD 2D PIC code “Smilei” and a pseudo-spectral 2D PIC code “Shockapic”.// Dispersion relations of light waves from PIC codes :

FDTD, “Smilei”

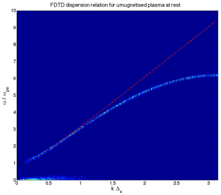

Spectral, “Shockapic”

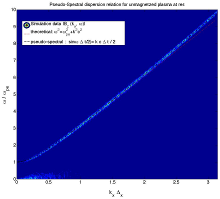

Both + theoretical :

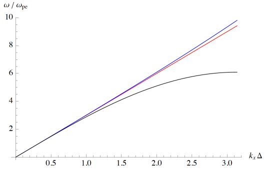

- In theory we should get $\omega^2 = \omega_{pe}^2 + k^2 c^2$ for a light wave in an unmagnetized plasma. Significant deviation for FDTD solvers, more subtle for Spectral solvers
- The difference is less obvious on the other proper plasma wavemodes (Whistler, Langmuir, Bernstein modes)
- Different techniques to mitigate the spurious grid-Cerenkov instability

Simulations setup

Shock is initiated by reflection of a cold $e^- - e^+$ beam on a reflecting wall at the right boundary (piston method) → interaction of two beams is unstable and bulds a shock as seen from the shocked plasma restframe.

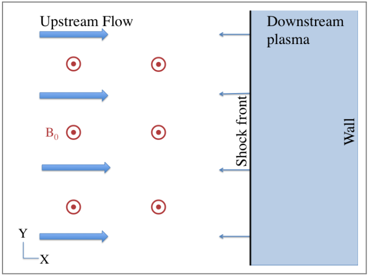

- Time : Simulations done up to $2000\omega_{pe}^{-1}$ and $< 500\omega_{pe}^{-1}$ with the *Smilei* and *Shockapic* codes, respectively (Sironi et al 13. : $> 10^4\omega_{pe}^{-1}$)
- Resolution : grid size is $\simeq \delta_e/4$ and the box transverse size $\simeq 256\delta_e$
- Noise : 20 part./cell (2 for *Shockapic*)
- Grid : 20 simulations exploring $\sigma \in [10^{-6}, 0.1]$ with each code. Complemetary $\sigma = 0$ and > 0.1 runs.

Global structure for different σ (I)

Density maps of $\gamma_0 = 10$ shocks at $t\omega_{pe} = 300$

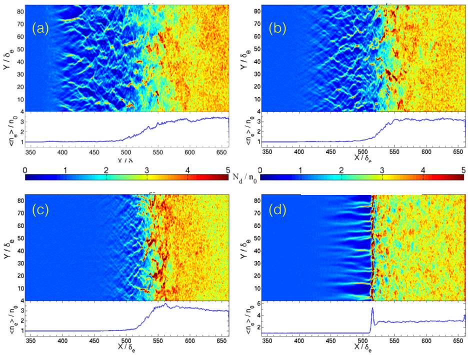

$\sigma = 10^{-5}$ (a), 10^{-4} (b), 10^{-3} (c) and $3 \cdot 10^{-2}$ (d).

- Shock front thickness $\simeq 10 - 50\delta_e$
- $\sigma = 0$ (a) : Weibel-filamentation governed shock structure.
- At intermediate $10^{-5} < \sigma < 10^{-2}$ (b,c) : the filaments in the precursor are slightly oblique. The precursor lengthscale is governed by the upstream magnetic field amplitude. About a Larmor radius of returning particles with energy $\gamma_0 m_e c^2$: $\ell_p \sim R_L = \gamma_0 m_e c^2/(eB_0)$ (e.g. Lemoine & Pelletier 2010).
- For $\sigma > 10^{-2}$ (d) : no particle precursor, strong EM emission from the front (see, e.g. Gallant et al. 92). Overshoot structure at the front. Apparent filamentary structure dissapears in later simulation times.

Global structure for different σ (II)

Magnetic turbulence and phase-space structure as function of σ.

- Recover very similar structure to the one presented by Sironi et al 13

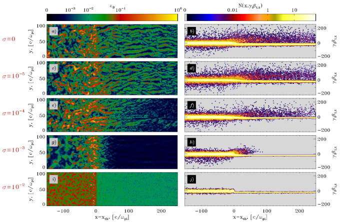

$\gamma_0 = 10$ shocks at $t\omega_{pe} = 2000$
Left $|B_z - B_{z,0}|$, Right : $x - p_x$.

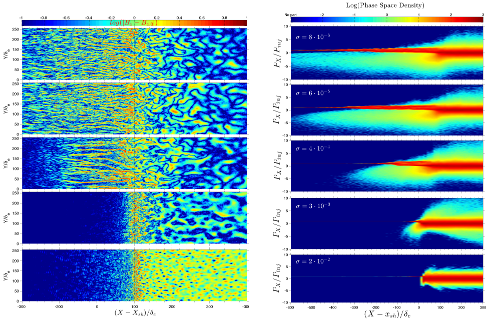

Shock Jump conditions : density

Compression ratio N_d/N_0 from simulations as function of σ.
Solid lines : ideal MHD prediction from conservation laws expressed in the downstream frame.

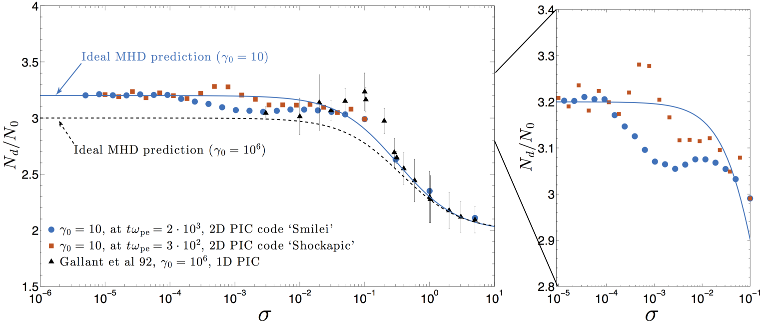

At low $\sigma < 10^{-4}$ consistent with the unmagnetized jump $[\Gamma_{ad} - 1](\gamma_0 - 1)/(\gamma_0 \beta_0)$ (Blandford & McKee 76, Kirk & Duffy 99, Spitkovsky 08). At high σ, $N_d/N_0 \to 2$.
Notable deviation when $10^{-4} < \sigma < 0.1$.

Front speed

Derivation of the MHD front speed as seen from the downstream (strong shock limit) gives

$$\beta_{\rm f} = \frac{2(\gamma_0 - 1)(\Gamma_{\rm ad} - 1) + \Gamma_{\rm ad}\gamma_0\sigma + \sqrt{8(\gamma_0^2 - 1)\sigma(1+\sigma)(2-\Gamma_{\rm ad}) + [2(\gamma_0 - 1)(\Gamma_{\rm ad} - 1) + \Gamma_{\rm ad}\gamma_0\sigma]^2}}{4(1+\sigma)\sqrt{\gamma_0^2 - 1}}$$

→ Consistent with Spitkovsky 08 in $\sigma = 0$ limit and with Kennel & Coroniti 84, Lemoine et al 16 for $\Gamma_{\rm ad} = 4/3$ (3/2 here because 2D plasma). For $\sigma > 1$, $\beta_{\rm f} \to 1$.

Comparison with simulations :

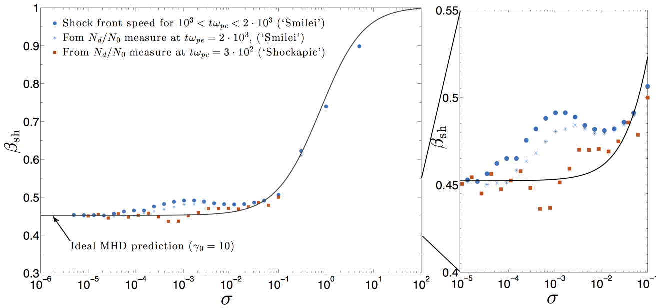

Shock formation timescales

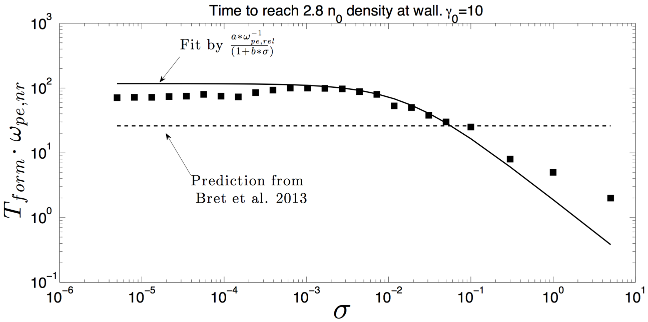

→ $T_{\text{form}} \propto \omega_{\text{pe,rel}}^{-1} \propto \sqrt{\gamma_0}\omega_{\text{pe}}^{-1}$ for all σ

→ $T_{\text{form}} \propto \omega_{\text{pe,rel}}^{-1}/\sigma$ when σ close to unity

Case of a $\sigma = 10^{-5}$ shock

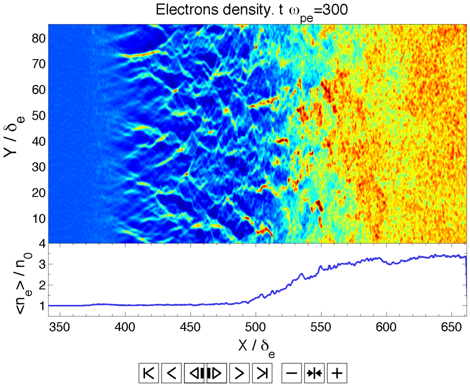

- Well-studied case (Silva et al. 03, Spitkovsky 08, Sironi et al 13, Bret et al 13)
- Initial flows overlap is Weibel-filamentation unstable at a $\sim \delta_e \sqrt{\gamma_0}$ scale.
- Currents reach the Alfven limit and build up the shock (magn. energy grows up to the level when the oncoming flow is stopped)
- Precursor beam of reflected/accelerated electrons → Weibel structured precursor by interaction of hot beam with cold upstream flow

Case of a $\sigma = 10^{-3}$ shock

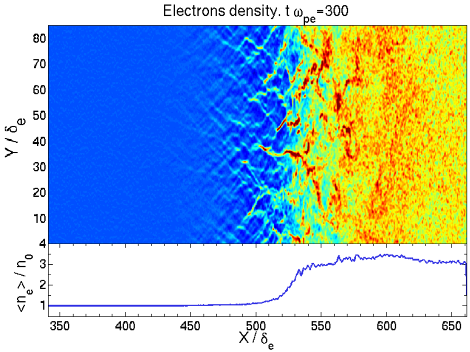

- Mixed case. Filamentation still dominant but accumulation is observable at the tip of the reflected flow.
- Slightly oblique filaments
- Measurable rms perp current in the precursor.

Case of $\sigma \geq 0.01$ shocks

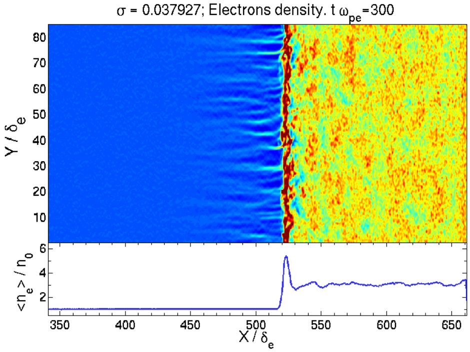

Evolution of $J_\perp$ for a $\sigma = 0.01$, $\gamma_0 = 30$ shock.

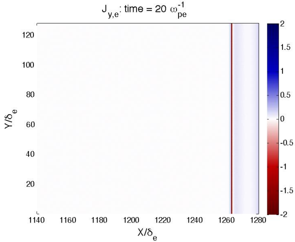

Density accumulation at the tip of interpenetrating beams → Shell kicked towards downstream if pressure is not sufficient to support the shock front. Oblique filametation (if possible) in the downstream forming region during shock formation.

Theoretical challenges

While the shock formation for a $\sigma = 0$ shock was conveniently described by Bret et al 13 and a model of a $\sigma \gg 1$ shocks is described by Alsop & Arons 88, Gallant et al. 92, the case of $0 \ll \sigma < 1$ is more involved

Transverse to $\vec{B}$ plasma fluctiations for $\omega_{ce}/\omega_{pe} = 0.5$

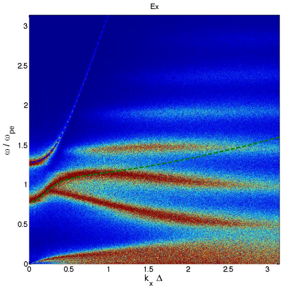

- $\rightarrow$ Importance of the fluctuations study and beam-type instabilities
- X-mode (coupled to Bernstein modes) $\rightarrow$ Maser-synchrotron $\rightarrow$ Parallel to shock normal but involves transverse to $\vec{B}_0$ modes.
- Filamentation, aperiodic instability $\rightarrow$ Perp to the shock normal and to $\vec{B}_0$.
- Convenient description needs to account for both with growing σ
- Role of third dimension in the shock structure ?(e.g. Simulations of Sironi et al 13)

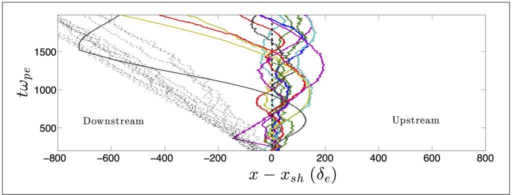
1500
1000
500
$t\omega_{pe}$
Downstream
Upstream
−800
−600
−400
−200
0
200
400
600
800
$x - x_{sh}$ (δ_e)

Downstream distribution for diff. magnetizations

Downstream distribution functions $f(\gamma)$

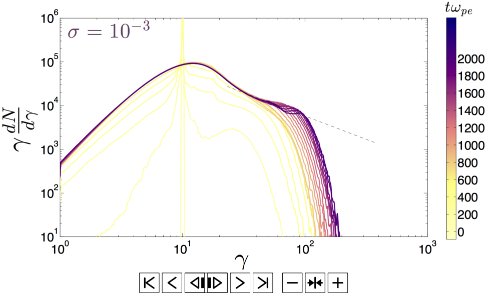

- For $\sigma \leq 10^{-4}$, acceleration similar to the unmagnetised shocks.
- For $\sigma \leq 10^{-3}$ slightly more rapid acceleration, but saturation energy reached at $t\omega_{pe} = 2000$.
- For $\sigma \geq 10^{-2}$ no supra-thermal component.
- Power-law tail index $s \simeq 2.$?

Maximal energy in time

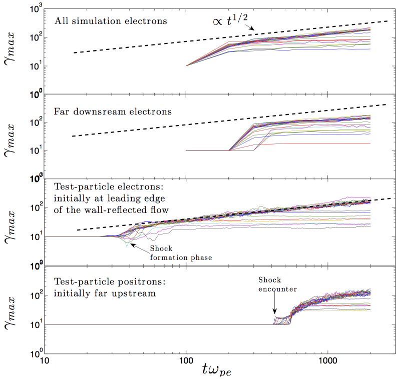

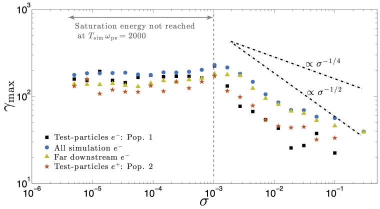

- $\gamma_{max} \propto t^{1/2}$ recovered, as found in Stockem et al. 11, Sironi et al. 13
- … γ_{max} is not saturated for $\sigma < 10^{-3}$ at the simulations end $= 2000\omega_{pe}^{-1} \simeq 600\omega_{pe,rel}^{-1}$. Probably not sufficient to fill the acceleration box and arrive to the saturation energy (as demonstrated by Sironi et al. 13).

Test-particles kinematics downstream (I)

Downstream turbulence → Static decaying microturbulence.
Particles injected from the wall at $t\omega_{pe} = 500$ with $\vec{p} = p_x\vec{n}$
→ Experience downstream decaying turbulence.

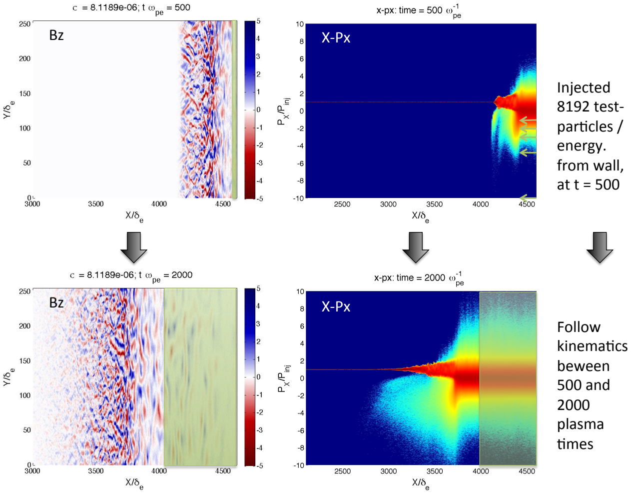

Test-particles kinematics downstream (II)

Diffusion coefficient in the shock propagation direction (Perp. to $\vec{B_0}$)

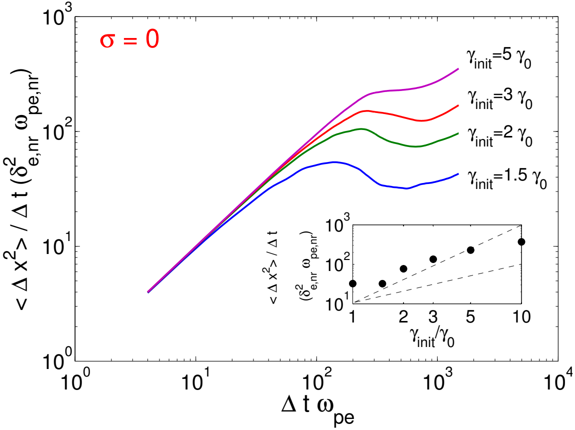

Diffusion effectively reached but $D_\perp \propto \gamma_i^2$ is not obvious.
Also the diffusion 'plateau' is not asymptotic...

Test-particles diffusion for increasing σ

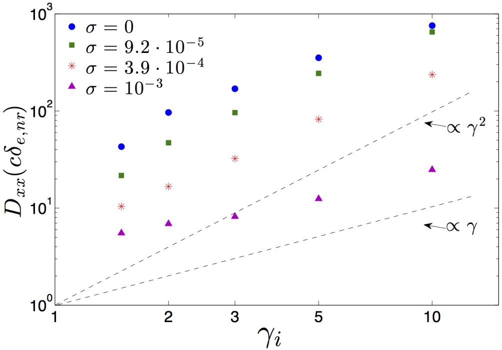

$D_\perp$ saturation for increasing σ. Result of lower turbulence $\delta B^2/B_0$ level or tighter turbulence region ?

Energy diffusion

In a simple form the Fokker-Plank equation for the shock swepted particles writes

$$\frac{\partial f}{\partial t} = \frac{\partial}{\partial \gamma}\left[\mathbf{D}\cdot\frac{\partial f}{\partial \gamma} - \mathbf{A}f\right] \qquad (1)$$

$D = \langle \Delta\gamma^2 \rangle / \Delta t$ is the momentum diffusion term responsible for the isotropic part of f (e.g. Moiseev & Sagdeev 63). Second order in energy.
A is the drag term → First order term.

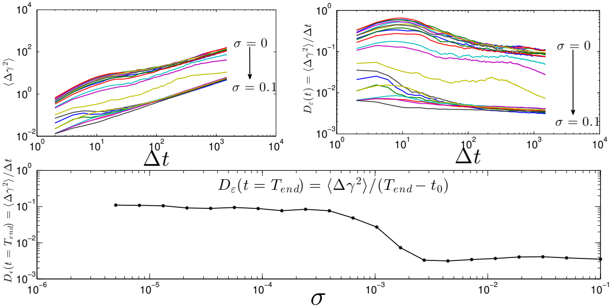

→ Clear transition between $\sigma = 10^{-3}$ and $\sigma = 10^{-2}$

Summary and further ideas

1. Shock structure follows the description by Sironi et al 13, but the precursor structure need a careful attention (importance of perp. current with growing σ, e.g., Lemoine et al. 14 and suppelementary analysis here).
2. Shock jump conditions and speed satisfactorily explained by the ideal MHD for $\sigma < 10^{-4}$ and ideal MHD-EM precursor for $\sigma > 0.1$. Deviation at intermediate σ.
3. Shock formation ... at $\sigma < 10^{-4}$ unmagnetized approx. is ok (framework described by Bret et al. 13).
4. Requirement for a general formalism at arbitrary magnetization. Theoretically involved because of transverse filamentation is competing with beam cyclotron instability. Also the problem is not periodic. Note that a current-based approach is presented in Lemoine et al. 14
5. Maximum particle energy $\propto \sqrt{t}$, in consistency with Sironi et al. 13. But $\gamma_{max} \propto \sigma^{-1/2}$ here, at shorter simulation times. While $\propto \sigma^{-1/4}$ in long simulations ($> 10^4 \omega_{pe,rel}^{-1}$).
6. Downstream particle diffusion scales as E^2 in weakly magnetized shocks but does not hold at intemediate σ. Eventually no diffusion for $\sigma > 10^{-2}$.
7. Clear transition seen between $\sigma = 10^{-3}$ and $\sigma = 10^{-2}$ shocks.